X-615-68-316

PREPRINT

NASA TM X- 63315

SOUNDING ROCKET MEASUREMENTS OF ION COMPOSITION AND CHARGED PARTICLE TEMPERATURES IN THE TOPSIDE IONOSPHERE

E. J. R. MAIER

AUGUST 1968

GSFC

GODDARD SPACE FLIGHT CENTER

GREENBELT, MARYLAND

SOUNDING ROCKET MEASUREMENTS OF ION COMPOSITION AND CHARGED PARTICLE TEMPERATURES IN THE TOPSIDE IONOSPHERE

E. J. R. Maier
Laboratory for Space Sciences
NASA Goddard Space Flight Center
Greenbelt, Maryland

ABSTRACT

The concentrations of H^+, He^+, and $(O^+ + N^+)$ were measured as a function of altitude from 300 km to 600 km by means of an ion mass spectrometer. The major constituent was found to be O^+ over the entire altitude range, decreasing from >99% of the total ion density at 300 km to 88% at 600 km. Hydrogen and helium ions were present as minor constituents increasing with altitude to 11% and ~1% respectively at 600 km. At the same time, the electron and total ion densities and temperature were measured and compared by means of retarding potential analyzers. The ion temperature was found to increase with an altitude gradient of 1.7^{o}/km from 1100^{o} at 300 km to 1600^{o} at 600 km. Electron temperatures were found to increase rather sharply in the 400 to 500 km altitude from the fairly typical value of 2500^{o} to the very high value of 3500^{o} at 600 km. Comparisons with the electron density profiles obtained from the Wallops Island ionosonde station and from the topside sounder Alouette II showed good agreement. Relationships among the observables, and with the inferred neutral gas temperature of 1060^{o} are discussed. The ARGO D-4 rocket carrying the payload was launched from Wallops Island, Virginia, at 15:29 hours, local time October 6, 1966.

INTRODUCTION

A complete description of the upper ionosphere involves solution of the continuity and energy conduction equations under suitable boundary conditions for a rather large number of variables. Variations of the basic energy input provided by the sun occur both "randomly" - e.g. some solar disturbances - and coherently, the more evident variations having the diurnal, seasonal, and solar cycle periodicities. Observations provided by experiments carried on satellites can provide specification of some of the average boundary conditions at particular altitudes, but cannot provide vertical profiles of the parameters for a particular time. Comprehensive vertical soundings of the ionosphere are essential to correctly assess the validity of theoretical descriptions of the chemistry and energy exchange within the upper ionosphere and it is toward this end that the present research is directed. A recent review of this field is given by Bauer (1968).

The history of in situ observations of the ionosphere began relatively recently, but by present measures there has been only a small amount of vertical sounding data obtained compared, e.g., to the many hours of satellite data already published. In addition to paucity of data, the interpretation of vertical sounding results is further complicated by the fact that the difficulty of some of the experiments has not allowed measurement of more than several

of the significant parameters by a particular payload. Although it is still not possible for a single payload to obtain measurements from, say, the D region to the lower exosphere, it is possible to obtain measurements over a significant fraction of that altitude interval. The objectives of the present experiment were to measure the ion composition of the major and light minor ions as well as the electron and ion temperatures and their total concentration in the region from the F layer to payload apogee. The results presented here were obtained from NASA payload 8.38 launched from the Wallops Island, Virginia facility at 15:29 EST, October 6, 1966. An altitude of 640 km was obtained by the payload of the ARGO D-4 rocket.

Direct observations of the ionosphere have traditionally been suspect because of the possibility of contamination of the environment by outgassing from heated rocket components such as the nose cone or last stage casing. To minimize this possibility the payload was separated from the 4th stage by means of the standard separation device available for the D-4. The standard fiberglass noise cone used with the D-4 was deployed forward of the payload to uncover the various experiments. To prevent the sampling of the nose cone wake and outgassing products a weight was deployed from the separated nose cone to place it in a ballistic trajectory slightly different from that of the payload.

II. INSTRUMENTATION

The payload instrumentation consisted basically of 5 experiments: 1. a medium resolution mass spectrometer capable of scanning the mass range from 1 to 20 AMU. 2. A planar electron retarding potential analyzer. 3. A planar Langmuir probe. 4. A planar ion retarding analyzer. 5. A VLF receiver and plasma stimulus experiment instrumented by R. E. Barrington of the Defence Research Telecommunications Establishment, Canada.

The mass spectrometer was of the Wien velocity filter type similar to the instrument used by Ogilvie et al (1968) for observations of H^+ and He^{++} energy spectra. In this device, the detected particles are those which traverse a straight line trajectory through crossed electric and magnetic fields. To use this type of instrument for mass discrimination of low energy ions, it is necessary to accelerate all the ions to some appropriate energy (400eV) such that the resultant velocity spread, proportional to $m^{-\frac{1}{2}}$, can be observed as a measure of the mass of the ion. A diagram of the instrument is shown in Fig. 1. With a fixed magnetic field of 1100 gauss, and an ion energy of 400eV, the electric field required to scan the mass range from 0.5 to 25 AMU was provided by a sweep voltage which decreased exponentially from 1400 volts to 200 volts in 10 seconds. Note that the swept electric field region and the magnetic field region are completely contained within the magnetic yoke which is at -400 volts

with respect to the payload structure. Thus the leakage fields interacting with the ambient medium are constant throughout the mass sweep of the instrument. Mass selected ions were detected by means of an electron multiplier at the exit aperture of the velocity selector. As shown in Fig. 1, the entire spectrometer and electron multiplier assembly was contained in an evacuated chamber. A one inch opening was uncovered when the payload reached an altitude of 200 km, exposing the -5 volt ion draw in plate containing the entrance aperture. To facilitate the pre-flight calibration procedure and to accommodate the electronic components contained within the spectrometer vacuum assembly, a 1 liter/sec vac-ion pump was kept operating from well before launch until front cap deployment so that valid data could be obtained immediately, without a delay for the spectrometer to pump down to the ambient pressure.

The ion and electron retarding analyzers were of the planar multi-gridded type similar to those used by other investigators (Bourdeau et al, 1961). The sweep voltage excursion was three volts, for the electron trap ranging from -1 to +2 volts, and applied to the outer grid, whereas for the ion trap it ranged from 0 to +3 volts and was applied to the grid behind the grounded outer grid. Several precautions were taken to preclude distortion of the response functions of the retarding analyzers as a result of the vehicle potential shifts caused by the variations of potentials on exposed electrodes.

The retarding voltages for the two traps were held constant, and then varied linearly with time, with an appropriate phase shift such that while one sweep was developing the retarding function the sweep on the other trap was held at a constant potential. In addition to isolating trap interactions, the constant potential portions of the sweep functions permit study of attitude dependence of the observed currents. Operation of the VLF stimulus will not be discussed in this paper other than to mention the interaction with the retarding analyzer. The 20 inch stimulus antenna was excited by a short, high amplitude pulse followed by a VLF sweep of about 20 volts amplitude. A "chopping" of the trap response currents occurred as the stimulus sweep frequency passed within the bandpass of the retarding analyzer electrometers and their subcarriers, enabling observation of a variation in vehicle potential which was presumably present at all times during application of the stimulus potential. In anticipation of this effect, the VLF stimulus was operated at a low (20%) duty cycle to enable selection of retarding analyzer data obtained when the stimulus was off.

III. DATA REDUCTION

The payload was not despun so that spin stabilization of the payload would be effective throughout much of the up leg of the trajectory, after which angular momentum coupled into payload body axes other than the axis of symmetry. To reduce the angle between the spectrometer axis and the velocity vector, the spectrometer was inclined 8^{o} from the nominal spin

axis of the payload. Thus, the spectrometer scanned an 8^{o} half angle cone about 4 times each second. The mass scan time of 10 seconds was selected to insure data at each mass of interest for the most-forward looking direction of the conical surface scanned. This spin modulation of each of the mass peaks enabled selection of the appropriate measurements for which the spectrometer axis was almost along the payload velocity vector. As expected, the depth of the spin modulation within each of the mass peaks was mass dependent and varied with position along the vehicle trajectory. The ratio of the maximum observed current to the minimum observed current varied from $\approx$1 and 1.5 for H^{+} and 0^{+} respectively at 330 km to 1.5 and 5 at 600 km. On the down leg of the flight the payload precession became more severe causing the "forward looking" experiments to scan a very large range of angles with respect to the velocity vector. Thus the maximum current ratios became 2 for H^{+} and 200 for 0^{+}. These current ratios are consistent with the interaction of the payload velocity, the angle of attack, the moderate (5 volt) draw-in-potential, and the higher thermal velocity for protons as compared to that for 0^{+} ions at a comparable temperature. Figure 2 is a plot of the spectrometer output current as amplified by the electron multiplier. Data presented were obtained when the payload was looking most nearly along the velocity vector. The downleg data included

are not used in the following discussion but are presented to illustrate the onset of attitude-dependent deviations.

The electron trap response curves were used to determine both the electron density profile and the electron temperature profile. Bourdeau et al (1961) and others have used the relation $I = \alpha\, Ne\, \bar{v}/2\sqrt{\pi}$ to relate the effective grid transparency α, the electron density N, and the mean thermal velocity $\bar{v}$ to the observed current I in the "saturation current region" of a planar retarding analyzer response function. Using a value for α of 0.65 resulted in an electron density at 250 km agreeing well with the result obtained from the Wallops Island ionosonde station for the electron density at F_{max}. Electron temperatures were obtained in the standard manner from the logarithmic decrement of the current response with applied retarding voltage. Ne and Te are shown in Figures 3 and 4. The electron density profile for the descent part of the flight was in good agreement with that shown in the figure for the ascent. As can be seen, the change in the electron temperature gradient in the altitude interval 400-500 km was substantiated by the descent leg data.

Also included in Figure 4 is an electron temperature measurement obtained by J. Donley (private communication) from an experiment on Explorer 31. A temperature of 3800^{o} at 1100 km over the Wallops Island launch site was observed on 8/15/66 at a local time comparable to that of the launch.

Analysis of the ion response characteristic was carried out on the assumption that the various ion species were at the same temperature. Slight differences between the temperature of H^+ and O^+ or slight deviation of the H^+ velocity distribution from Maxwellian as calculated by Banks (1968) will have little effect on the response curve.

The observed curves were compared to the theoretical curves for the responses of the planar retarding analyzer to a multi-constituent plasma (Bourdeau et al, 1961) using a transparency factor X=0.85. The various constituents were taken to be present in the percentages measured by the spectrometer and good agreement was obtained for the ion temperatures and densities as given in Figures 3 and 4. Inclusion in the theoretical function of terms for small admixtures of molecular ionic species did not significantly alter the fit to the data and it is judged that there was no significant molecular component above 300 km for the case in question.

IV. RESULTS AND DISCUSSIONS

Figure 5 shows the altitude dependence of the densities of the three species observed. Because the resolution of the spectrometer was not adequate to resolve O^+ and N^+, the curve for the heavy atomic species represents the sum of the concentrations of O^+ and the relatively minor, but possibly significant species N^+.

The absolute sensitivities of the instrument for the mass range of interest were measured in the laboratory over the energy range 20 eV to 200 eV using separated ion beams. Using the extrapolation of these curves to 10 eV, it was found that the sensitivity for H^+ was about 0.6 times that for O^+. This ratio is (accidentally) close to the inverse of that expected via the enhanced coupling of light ions as a consequence of their higher ratio of thermal velocity to rocket velocity. Hence the basic currents measured have been regarded as proportional to the ambient density and have been converted to density by normalizing to the ionogram result at F_{max}.

There are a number of interesting features evident in the altitude distributions of Figure 5. Atomic oxygen ions were the major constituent at all altitudes observed. Hydrogen ions were present throughout the flight, their concentration increasing to 9000 ions cm^{-3} (0.11 N_e) at 600 km. Helium ions were detectable above 430 km, but their concentration never exceeded 1% of the total charged particle content. In addition to the rocket data, some points from a topside sounder profile recorded on August 5, 1966 and analyzed by J. E. Jackson (private communication) are shown as circles in Figure 5. The sounder data, obtained at a corresponding latitude and time, show a topside scale height of 150 km, in agreement with that of the present measurement.

The Kp indices for August 5 and October 6, 1966 were, respectively, 18 and 27, implying comparable activities and neutral gas temperatures for this time of rising solar activity. Brace et al (1968) have presented results from Explorer 22 describing the general (daytime) increase of electron density and temperature at ≈1000 km altitude during three years of the increasing activity phase of the solar cycle. The data which they present were obtained in January of the years 1965, 1966 and 1967 and thus are not directly comparable with the present data due to the different solar zenith angles in the northern latitudes, but the general agreement is good if our density and temperature profiles are extrapolated to 1000 km. It should be mentioned that the plasma parameters at middle to high latitudes are especially sensitive to short term variations of energy input as evidenced, for example, by the variations within the January 1967 data presented by Brace et al (1968) in their Figures 1 and 2.

Bauer (1964) has pointed out that a study of the ratios of H^+ concentration to the concentration of other ions can often be more informative than the absolute measurements themselves. For example, systematic errors associated with the coupling between the plasma and the spectrometer will tend to cancel, resulting in greater accuracy in the determination of the ratios of the concentration. In addition, many expected altitude dependences of partial concentrations contain identical terms involving the temperature gradients. Thus

some terms will cancel in the ratio, and it may be possible to more clearly distinguish the dominant controlling process. Equation 1 is the expression for H^+ concentration if charge exchange with 0 is the controlling reaction (Hanson and Ortenburger, 1961).

$$n(H^+) = \frac{9}{8} \frac{n(H)}{n(0)} n(0^+) \tag{1}$$

Thus although $n(H^+)$ depends on the altitude distribution of both the neutral gas and 0^+, the ratio

$$\frac{n(H^+)}{n(0^+)} = \frac{9}{8} \frac{n(H)}{n(0)} \propto \exp\left[\frac{(M_{0^+}-M_{H^+})gz}{k\ T_n}\right] \tag{2}$$

is a function only of the temperature of the neutral gas, T_n, and the geopotential energy. In this expression M_{0+} and M_{H+} denote the masses of atomic oxygen and hydrogen, g is the gravitational acceleration, z is the altitude, and k is the Boltzmann constant.

The left curve of Figure 6 is a plot of the $H^+/0^+$ ratio vs. payload altitude. From the observed constant scale height* of 58 km from about 300 to 550 km, we conclude that if chemical equilibrium is obtained between hydrogen and oxygen the neutral gas temperature is 1040^o. This temperature is in excellent agreement with the neutral temperature of 1020^o given by Chandra and Krishnamurthy's (1968) model based on the 10cm flux and the planetary magnetic index for October 6, 1966.

---

*In this paper, the scale height is defined to include the sign of the exponent such that H>0 denotes a concentration increasing with altitude as exp(z/H).

The equilibrium equations for the forces on ions of masses m_j, assumed to be perfect gasses at the same temperature T_i, are:

$$\frac{dp_j}{dz} + n_j m_j g - n_j eE = 0 \tag{3}$$

where P_j is the partial pressure $n_j kT_i$ of species j, and E is the electric field. To solve for the altitude distributions of the various species requires the solution of these equations and a similar one for the electron parameters under the additional constraint of charge neutrality $n_e = \Sigma\, n_j$ (Mange, 1960; Bauer, 1966). Two of equations (3) for ion species 1 and 2 can be combined to eliminate the electric field, the result being

$$\frac{n_1}{n_2} \alpha \exp \left[\int \frac{(m_2-m_1)g}{k\, T_i}\, dz\right] \tag{4}$$

which depends only on the ion temperature, and not the electron or neutral gas temperatures. It has been observed by many authors that the diffusive equilibrium and chemical equilibrium scale heights for H^+ in 0^+ are identical. We point out, however, that this is true only for the case of thermal equilibrium between the ions and neutrals. Thus the departure near 550 km of the $n(H^+)/n(0^+)$ scale height (Fig. 6) from its value of 58 km at lower altitudes is evidence of the transition from chemical to diffusive equilibrium involving an ion temperature greater than the neutral gas temperature.

Applying equation 4 to the species H^+ and He^+, the ratio of the concentrations of these ions, for the case of diffusive equilibrium, is expected to increase with altitude as

$$R = \frac{N(H^+)}{N(He^+)} \alpha \exp \left[\int \frac{(M_{He^+} - M_{H^+})g}{k\, T_i}\, dz\right] \sim \exp \frac{z}{500} \tag{5}$$

From the right curve of Figure 6 it can be seen that there is a change of slope near 530 km with qualitative (and probably quantitative) agreement with a 500 km scale height above that altitude.

Returning now to consideration of the altitude profiles of the concentrations, Table I summarizes some of the observations which can be deduced from the data. We compare the observed scale heights (column 3) to scale heights calculated on the basis of as many as 4 different classes of theoretical altitude distributions (columns 4 thru 7). These are for, respectively, the appropriate chemical control equations, the diffusive equilibrium equations with or without the temperature gradient terms, and the altitude dependence including the effects of thermal diffusion as evaluated by Walker (1967).

The O^+ concentration was found to decrease with a scale height of -160 km in the altitude range from 350 to 550 km. Using the measured temperatures and measured temperature gradients in this region, we found a diffusive equilibrium scale height of -151 km. If the temperature gradient term is not included in the calculation, the resultant scale height if -254 km, in clear disagreement with the observation. Thus it can be concluded that, for these data, oxygen ions are in diffusive equilibrium if proper account is taken of all the terms in the diffusive equilibrium relationship and it is not necessary to invoke any parameters other than the

plasma composition and temperature. A similar conclusion has been reached by B. C. Narasinga Rao (1968) who presents an interpretation of data from a rocket launched into a considerably cooler neutral gas atmosphere.

Hydrogen ions follow a scale height of 90 km over the range from 350 to 450 km. This is in good agreement with the altitude dependence based on charge exchange with 0 as the controlling mechanism. At the higher altitudes, the observed scale height is in best agreement with that calculated based on diffusive equilibrium including the observed temperature gradients. The relatively low apogee did not allow us to conclusively exclude the possibility of thermal diffusion or a directed flow contributing to the altitude dependence.

Helium ions, first observed near 430 km at a density of 200 cm^{-3}, followed a scale height of 60 km. This is in qualitative agreement with the scale height calculated based on the reaction with N_2 (Bauer, 1966). At higher altitudes, the increasing density yields quickly to (at 500 km) an essentially constant density condition which obtains until payload apogee. The unfortunately low apogee does not allow us to comment on the helium distribution above this transition region.

Finally, we can briefly summarize the temperature results present in an earlier section. The electron temperature increased from about 2500^{o} at 300 km to 3800^{o} above 600 km, with a region of enhanced

temperature gradient from 400 to 500 km altitude. The measured ion temperature increased from about 1000^{o}, in agreement with both the inferred and model gas temperature at 300 km, to 1600^{o} at 600 km altitude. Thus at the apogee altitude attained by the payload the ions are not in thermal equilibrium with either the exospheric gas or the electrons. Banks (1967) has used the ion temperature fractional separation $X = (T_i-T_n)/(T_e-T_n)$ as a parameter in discussing the problem of ion temperature coupling within the ionosphere. For the data obtained from 8.38, X increases from essentially zero at F_{max} to 0.2 at 600 km. Thus these data are in the regime $X<\frac{1}{2}$ for which Banks found transport effects to be unimportant.

ACKNOWLEDGMENT

It is a pleasure to acknowledge discussions with Dr. S. J. Bauer concerning some aspects of the interpretation of this data.

REFERENCES

Banks, P. M., "Ion Temperature in the Upper Atmosphere" J. Geophys. Res., 72, 3365-3384, 1967.

Banks, P. M., "Hydrogen Ion Velocity Distributions in the Ionosphere", Planetary Space Sci., to be published, 1968.

Bauer, S. J., "Some Implications of a Direct Measurement of the Hydrogen and Helium Ion Distribution in the Upper Atmosphere", J. Geophys. Res., 69, 553-555, 1964.

Bauer, S. J., "The Constitution of the Topside Ionosphere", Electron Density Profiles in the Ionosphere and Exosphere edited by J. Frihagen, pp. 270-279, North Holland Publishing Company, 1966a.

Bauer, S. J., "Chemical Processes Involving Helium Ions and the Behavior of Atomic Nitrogen Ions in the Upper Atmosphere", J. Geophys. Res., 71, 1508-1511, 1966b.

Bauer, S. J., "Rocket and Satellite Experiments in the Magnetosphere", Handbuch der Physik, Vol. 49, III, 4, 1968, to be published.

Bourdeau, R. E., J. L. Donley, G. P. Serbu, and E. C. Whipple, Jr., "Measurements of Sheath Currents and Equilibrium Potential on the Explorer 8 Satellite", J. Astron. Sci., 8, 65-73, 1961.

Brace, L. H., H. G. Mayr and B. M. Reddy, "The Early Effects of Increasing Solar Activity upon the Temperature and Density of the 1000-Kilometer Ionosphere", J. Geophys. Res. 73, 1607-1615, 1968.

Chandra, S., and B. V. Krishnamurthy, "The Response of the Upper Atmospheric Temperature to Changes in Solar EUV Radiation and Geomagnetic Activity", Planetary Space Sci., 16, pp. 231-242, 1968.

Hanson, W. B., and I. B. Ortenburger, "The Coupling between the Protonosphere and the Normal F Region", J. Geophys. Res. 66, pp. 1425-1435, 1961.

Mange, P., "The Distribution of Minor Ions in Electrostatic Equilibrium in the High Atmosphere", J. Geophys. Res., 65, 3833-3834, 1960.

Ogilvie, K. W., N. McIlwraith and T. D. Wilkerson, "A mass-energy analyzer for Space Plasmas", Rev. Sci. Inst., 1968, to be published.

Rao, B. C. Narasinga, "Ion, Electron, and Neutral Temperatures Derived from Ion Composition Distribution", submitted to J. Geophys. Res., 1968.

Walker, J. C. G., "Thermal Diffusion in the Topside Ionosphere", Planetary Space Sci., 15, 1151-1156, 1967.

FIGURE CAPTIONS

Figure 1 - Diagram of the ion mass spectrometer as implemented for NASA 8.38.

Figure 2 - Spectrometer electron multiplier anode current for the three mass groups, H^+, He^+, and $(N^+ + O^+)$, for the upleg and part of the downleg of NASA 8.38.

Figure 3 - Electron and ion density profiles as measured by the retarding potential analyzer. Downleg data for the electron retarding potential analyzer, not shown for clarity, were in very good agreement with the upleg data. Ion trap results for the downleg differ from upleg as a consequence of the poor vehicle attitude.

Figure 4 - Altitude profiles of the electron and ion temperature as measured on NASA 8.38.

Figure 5 - Summary of the partial ion and total charged particle concentrations. The curve for $z < 260$ km, labeled ionogram, was obtained from an ionogram recorded at the Wallops Island ionosonde station during the time of the flight. The circles denote electron density data points obtained from an Alouette topside sounder ionogram which was recorded August 5, 1966.

Figure 6 - Altitude profiles of the ratios of ion concentrations as measured by the spectrometer on NASA 8.38.

Table 1 - Summary of observed and calculated scale heights for various parameters and altitude intervals.

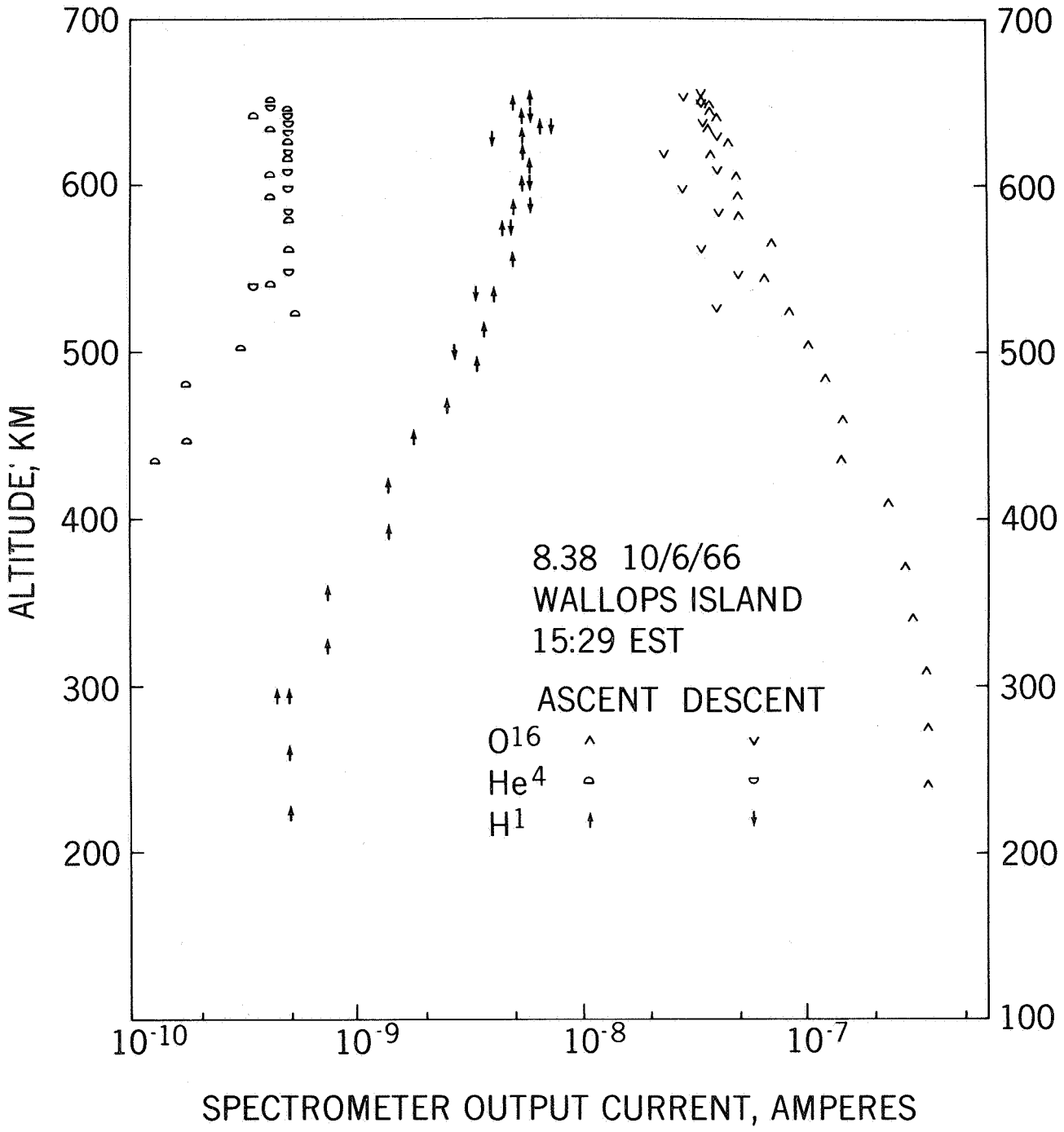
700
600
500
400
300
200
100
ALTITUDE, KM
8.38 10/6/66
WALLOPS ISLAND
15:29 EST
ASCENT DESCENT
O16
He4
H1
10-10
10-9
10-8
10-7
SPECTROMETER OUTPUT CURRENT, AMPERES

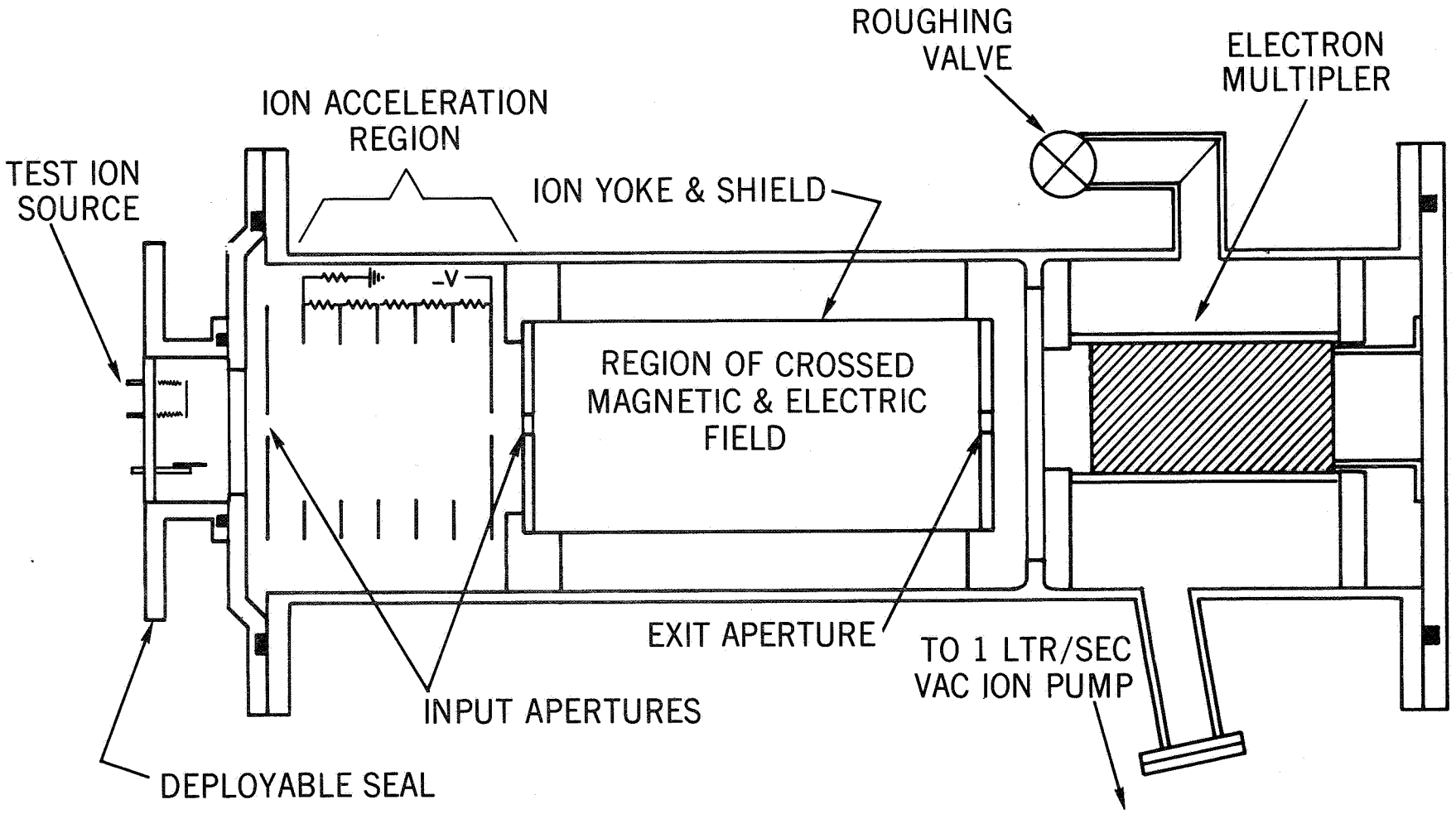
ROUGHING VALVE
ELECTRON MULTIPLER
ION ACCELERATION REGION
TEST ION SOURCE
ION YOKE & SHIELD
-V
REGION OF CROSSED MAGNETIC & ELECTRIC FIELD
EXIT APERTURE
TO 1 LTR/SEC VAC ION PUMP
INPUT APERTURES
DEPLOYABLE SEAL

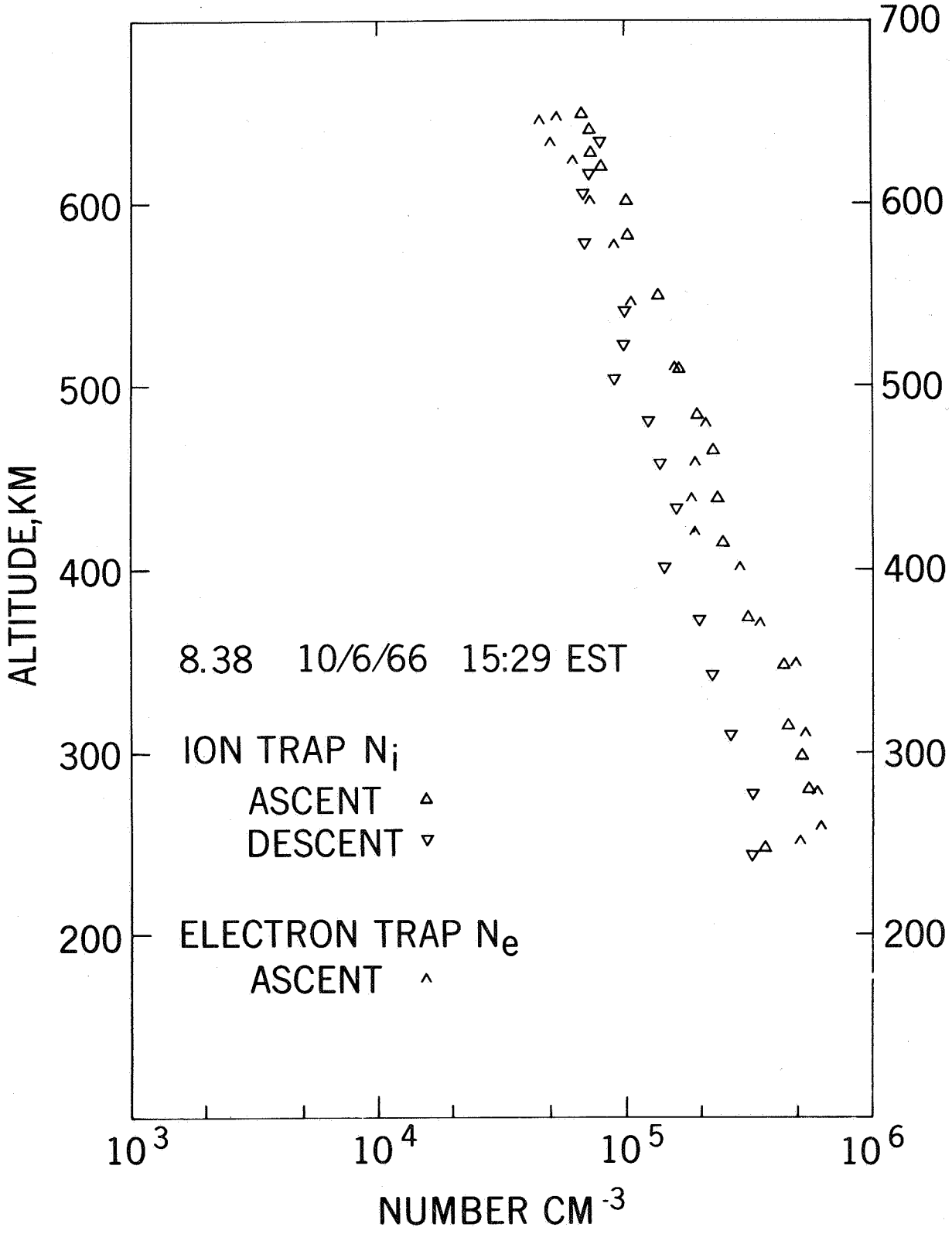
700
600
500
400
300
200
ALTITUDE,KM
8.38 10/6/66 15:29 EST
ION TRAP N_i
ASCENT
DESCENT
ELECTRON TRAP N_e
ASCENT
10^3
10^4
10^5
10^6
NUMBER CM^{-3}

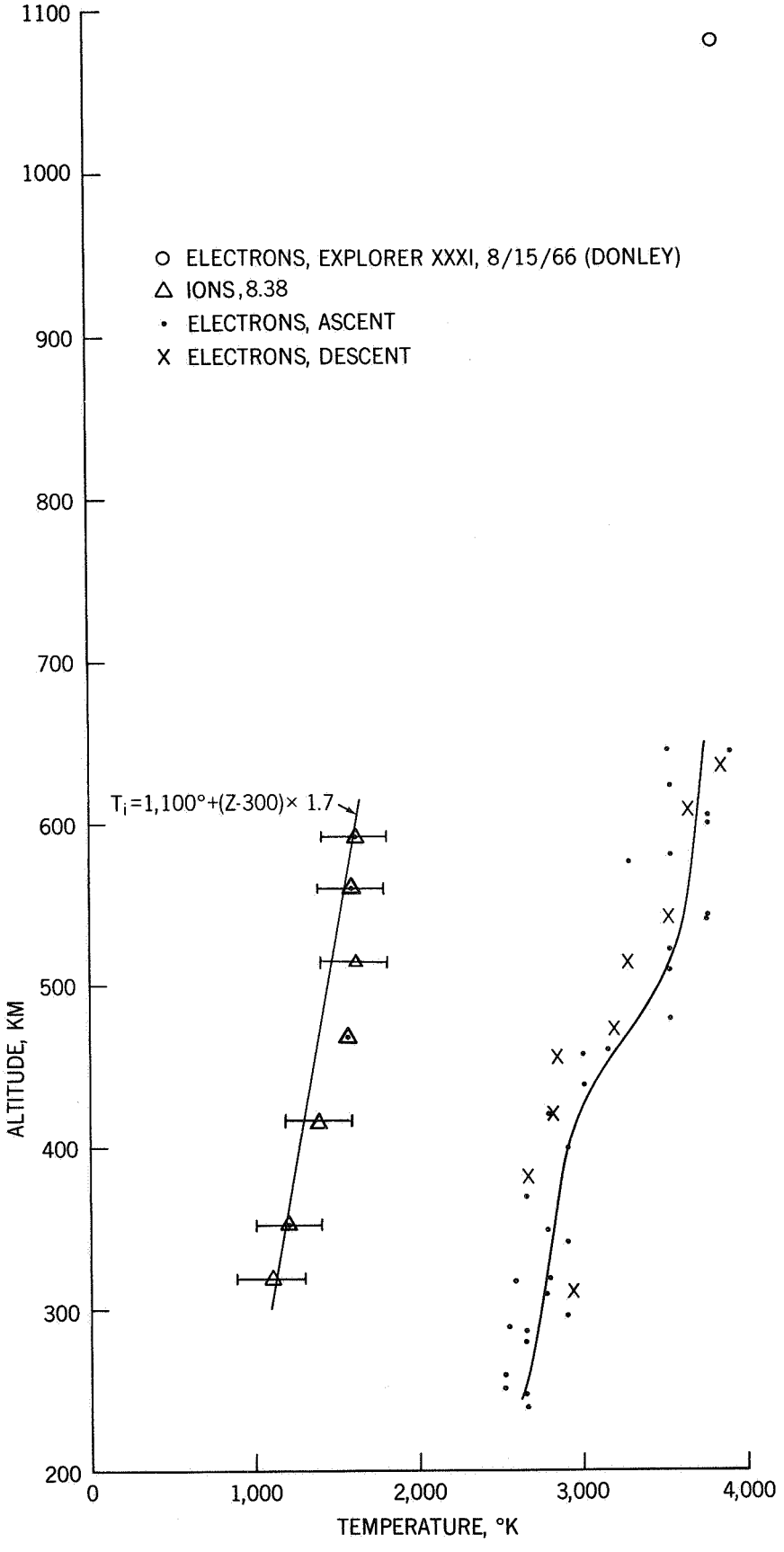
1100
1000
900
800
700
600
500
400
300
200
ALTITUDE, KM
0
1,000
2,000
3,000
4,000
TEMPERATURE, °K
O ELECTRONS, EXPLORER XXXI, 8/15/66 (DONLEY)
△ IONS, 8.38
• ELECTRONS, ASCENT
X ELECTRONS, DESCENT
T_i=1,100°+(Z-300)× 1.7

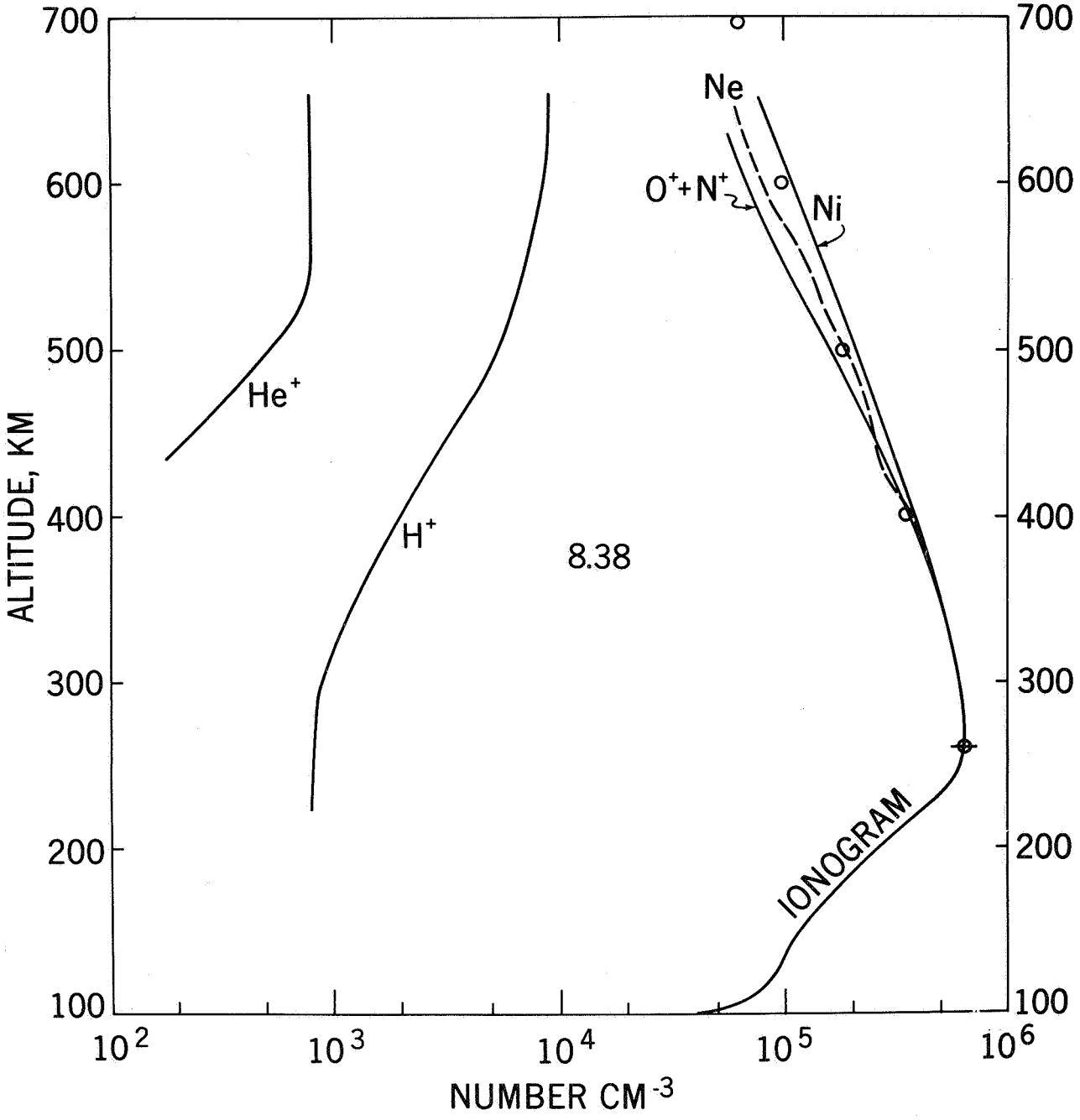
700
600
500
400
300
200
100
ALTITUDE, KM
He+
H+
Ne
O+ + N+
Ni
8.38
IONOGRAM
10 2
10 3
10 4
10 5
10 6
NUMBER CM -3

Measured Parameter	Altitude	Observed Scale Ht.	CALCULATED SCALE HEIGHTS				Conclusion
			Chemical Control	Diff. Equilib.	Diff.Equilib. w/o ∇T	Thermal Diff. Included (Walker)	
H^+/O^+	300-550	+58					T_n = 1040
O^+	350-550	-160		-151	-254		Diffusive equilibrium
H^+	350	+90	+89	342	267	830	Chemical control
	450	+90	+96	195	128	273	Chemical control
	600	175		167	148	213	Diffusive equilibrium with trend toward significant thermal diffusion
He^+	430-500	+60	+38	384	190	790	Chemical control
	>530	>3000		279	236	415	Transition altitude
H^+/He^+	>550	+500		460	460	460	Diff.eq.,independent of temp. gradient